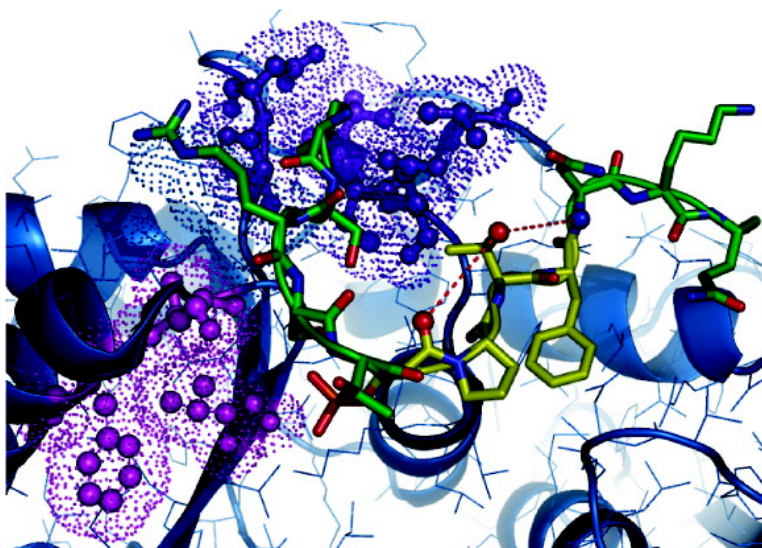


## Thermodynamics of Phosphopeptide Tethering to BRCT: The Structural Minima for Inhibitor Design

G. L. Lokesh, B. K. Muralidhara, Surendra S. Negi, and Amarnath Natarajan

*J. Am. Chem. Soc.*, **2007**, 129 (35), 10658-10659 • DOI: 10.1021/ja0739178 • Publication Date (Web): 09 August 2007

Downloaded from <http://pubs.acs.org> on February 15, 2009



### More About This Article

Additional resources and features associated with this article are available within the HTML version:

- Supporting Information
- Links to the 2 articles that cite this article, as of the time of this article download
- Access to high resolution figures
- Links to articles and content related to this article
- Copyright permission to reproduce figures and/or text from this article

[View the Full Text HTML](#)



**ACS Publications**  
High quality. High impact.

## Thermodynamics of Phosphopeptide Tethering to BRCT: The Structural Minima for Inhibitor Design

G. L. Lokesh,<sup>§</sup> B. K. Muralidhara,\*<sup>§,†</sup> Surendra S. Negi,<sup>#</sup> and Amarnath Natarajan\*<sup>§</sup>

Chemical Biology Program, Department of Pharmacology and Toxicology, Sealy Center for Structural Biology, University of Texas Medical Branch, Galveston, Texas 77555

Received May 31, 2007; E-mail: proteinmurali@gmail.com; amnatar@utmb.edu

In the post genomic era, protein–protein interactions have emerged as potential drug targets.<sup>1</sup> Unlike the well-defined active site structure of most enzymes, the protein–protein interaction interfaces are flat and expansive. Such a topology is adaptive and facilitates the heterologous interaction with multiple signaling partners that have similar structural motifs. Since the bulk of these interactions are intracellular, development of large druglike molecules that can span and compete for the protein–protein interface is not feasible because of permeability problems. Though protein–protein interactions share a large interface, there is a growing body of evidence that suggests that in these interactions the majority of the binding energy is contributed by a few amino acids at the interface. This indicates the possibility of a peptidomimetic approach for inhibitor design.<sup>2</sup>

The C-terminal domains of BRCA1 (BRCT) interact with phosphorylated proteins to regulate critical cellular functions in response to DNA damage. For example, the helicase BACH1, transcriptional co-repressor CtIP, and an ubiquitin-interacting motif containing protein Abraxas binds to BRCT domains in their phosphorylated form through a consensus recognition sequence pSXXF.<sup>3</sup> Structural analysis of the BRCT-phosphopeptide complex demonstrates identical binding modes for BACH1 and CtIP phosphopeptides. The phosphoserine (pS) of pSXXF motif is recognized by a shallow hydrophilic pocket on the N-terminus of BRCT domain, while the phenylalanine (F), the P+3 residue, recognizes a hydrophobic patch formed by residues from both BRCT domains (Figure 1).<sup>4</sup>

Since protein–protein interactions are transient, classical biochemical approaches do not provide the spatial and temporal control required to dissect the relevant signaling pathways. The use of small compounds to explore such transient interactions is emerging as a viable alternative. Our interests are to develop chemical probes/inhibitors to explore the role of BRCT mediated protein–protein interactions within the large BRCA1 signaling network. Toward this goal, here we report the use two complementary techniques to demonstrate that (1) tetrapeptides bind to BRCT with low-micromolar affinity, more importantly all four residues contribute to BRCT binding, and (2) the presence of a hydrophobic site close to the pSXXF site can be exploited for inhibitor design.

Using fluorescence polarization (FP) measurements we show that N-terminal labeling of a decapeptide containing the pSXXF motif is favored over C-terminal labeling (D1–3, Table 1).<sup>5a</sup> Using competitive binding FP studies we also show that the phosphate group on the serine and the phenyl ring on the phenyl alanine (P+3) is essential for the interaction of the peptide with BRCT (D4–6, Table 1). This observation is consistent with previously reported structural studies.<sup>4</sup> Truncation of the decapeptide D4 to a tetrapeptide T1 that shares the pSXXF motif, remarkably resulted in just a ~3-fold decrease in the inhibitor activity.

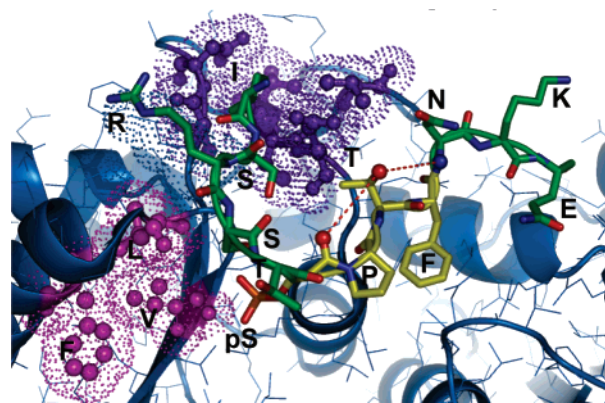


**Figure 1.** Packing interaction of BACH1 dodecapeptide with the BRCT domain (pdb:1T29).<sup>8</sup> All 12 residues are labeled and the minimal binding motif (pSPTF) is shown in yellow. The BRCT hydrophobic site constituted by Val<sub>1654</sub>, Leu<sub>1657</sub>, and Phe<sub>1662</sub> is shown in pink. The plausible intramolecular H-bonding of Thr with the backbone NH of the P+4 residue and CO of the P+1 residue is shown in red dotted-lines. The molecular graphic was generated using PyMol.<sup>9</sup>

**Table 1.** Thermodynamics of Peptide Mimics<sup>a</sup> Interaction with BRCT Domains Derived from Isothermal Calorimetric and Fluorescence Polarization Studies

	IC <sub>50</sub> <sup>b</sup> ( $\mu$ M)	K <sub>a</sub> × 10 <sup>-5</sup> (M <sup>-1</sup> )	- $\Delta$ G <sup>c</sup> (kcal/mol)	- $\Delta$ H (kcal/mol)	- $\Delta$ S <sup>c</sup> (cal/(mol K))
D1	103.66 <sup>c</sup>	0.31 ± 0.05	6.1 ± 0.2	20.9 ± 2.5	49.7 ± 3.3
D2	1.25 <sup>c</sup>	82.2 ± 5.6	9.4 ± 0.3	15.0 ± 0.2	18.6 ± 2.5
D3	0.45 <sup>c</sup>	97.1 ± 6.6	9.5 ± 0.3	14.9 ± 0.8	17.8 ± 1.4
D4	4.03 <sup>d</sup>	23.5 ± 1.7	8.7 ± 0.2	12.4 ± 0.3	12.4 ± 2.1
D5	> 300 <sup>d</sup>		no binding		
D6	> 300 <sup>d</sup>		no binding		
T1	13.82 <sup>d</sup>	3.2 ± 0.1	7.5 ± 0.2	10.7 ± 0.2	10.6 ± 1.5
T2	44.36 <sup>d</sup>	0.96 ± 0.08	6.7 ± 0.3	12.1 ± 0.2	17.9 ± 2.3
T3	70.87 <sup>d</sup>	0.21 ± 0.01	5.9 ± 0.2	14.7 ± 0.8	29.6 ± 3.4
T4	> 300 <sup>d</sup>		no binding		

<sup>a</sup> D1 = SRSTpSPTFNK( $\epsilon$ N-Flu)-CONH<sub>2</sub>; D2 = Flu-SRSTpSPTFNK-CONH<sub>2</sub>; D3 = Rod-SRSTpSPTFNK-CONH<sub>2</sub>; D4 = SRSTpSPTFNK-CONH<sub>2</sub>; D5 = SRSTpSPTFNK-CONH<sub>2</sub>; D6 = SRSTpSPTFNK-CONH<sub>2</sub>; T1 = pSPTF-CONH<sub>2</sub>; T2 = pSATF-CONH<sub>2</sub>; T3 = pSPAF-CONH<sub>2</sub> and T4 = EPTF-CONH<sub>2</sub>. <sup>b</sup> IC<sub>50</sub> values were determined by fluorescence polarization (see Supporting Information). <sup>c</sup> IC<sub>50</sub> values correspond to binding affinities for 1  $\mu$ M peptide. <sup>d</sup> IC<sub>50</sub> values are based on a competition FP assay with 100 nM of peptide D2 and 250 nM of BRCT. <sup>e</sup>  $\Delta$ G and  $\Delta$ S were calculated by the following equations, respectively:  $\Delta$ G = -RT ln K<sub>a</sub>;  $\Delta$ S = ( $\Delta$ H -  $\Delta$ G)/T.

The commonly used Glu substitution as a pSer mimic resulted in the complete loss of activity (T4, Table 1). To explore the effects of the side chains at P+1 and P+2 sites, we generated tetrapeptides T2 and T3 with corresponding Ala substitutions. Based on the IC<sub>50</sub> values, replacing the Pro at the P+1 site with Ala resulted in >3-fold loss of activity. The 3-fold loss of activity is equivalent to the loss of activity observed when the decapeptide (D4) was truncated to the tetrapeptide (T1). More interestingly replacing the Thr at

<sup>§</sup> Department of Pharmacology and Toxicology.

<sup>#</sup> Sealy Center for Structural Biology.

<sup>†</sup> Current address: Pfizer Global Biologics, St. Louis, Missouri 63017.

the P+2 site with Ala resulted in >5-fold loss of activity. This suggests in the context of the tetrapeptides the Thr side chain (P+2) is more important than the Pro (P+1) for BRCT binding. These observations are consistent with a previous oriented peptide library screen using decapeptides.<sup>5b</sup>

Using thermodynamic signatures derived from isothermal titration calorimetry (ITC) we have dissected the origin of differential BRCT affinities of deca- and tetrapeptides using a systematically designed peptide library (Table 1) with a structural perspective. On the basis of the association constants, the binding of BRCT to the N-terminus fluorescent labeled decapeptides is favored by ~300-fold compared to the C-terminus labeled decapeptide (**D1**–**3**; Table 1). The thermodynamic signatures ( $\Delta G$ ,  $\Delta H$ , and  $\Delta S$ ) are remarkably similar for the decapeptides (**D2** and **D3**), essentially not distinguishing the two different hydrophobic fluorophores (fluorescein and rhodamine) with similar hydrogen-bonding capabilities. It is also interesting to note that the N-terminus fluorescently labeled peptides have ~4-fold higher affinity for BRCT compared to the unlabeled peptide (**D2** and **D3** vs **D4**). This suggests the presence of a potential hydrophobic site adjacent to the pSXXF binding site occupied by Ile in the crystal structure (Figure 1, purple).

When the BACH1-bound (pdb:1T29) and unliganded (pdb:1JNX) BRCT structures<sup>4c,6</sup> are compared, a strikingly large hydrophobic pocket formed by Val<sub>1654</sub>, Leu<sub>1657</sub>, and Phe<sub>1662</sub> cluster was found (Figure 1, pink). The apolar surface area of this cluster was calculated<sup>7</sup> and was found to decrease by 25 Å<sup>2</sup> upon BACH1 binding, driven by the dip in the backbone of Leu<sub>1657</sub> forming a nice hydrophobic cavity (the C $\alpha$  rmsd between the structures is <0.5 Å). Independent docking simulations with fluorescein and rhodamine (labels) showed preferential affinity to this site over the N-terminal Ile site of the dodecapeptide in the crystal structure (Figure 1; also see Figure S7 of Supporting Information). The requirement of both N- and C-terminal BRCT domains for efficient phosphopeptide binding brings this hydrophobic pocket within striking distance of ~5 Å from the phosphate anchor site and can be exploited during inhibitor design. The non-phosphorylated (**D5**) and the Phe to Glu mutated (**D6**) peptides did not show any binding to BRCT, consistent with the FP data.

Next, ITC studies with BRCT and the tetrapeptides (**T1**–**4**) revealed that Glu substitution at pSer (**T4**) resulted in no binding, Ala substitution for Pro at P+1 resulted in a > 3-fold loss of activity (**T1** vs **T2**, Table 1), and replacement of Ala substitution for Thr at P+2 resulted in >15-fold loss of binding to BRCT (**T1** vs **T3**, Table 1). To explain these significant differences we took a closer look at the thermodynamic signatures. The strikingly similar  $\Delta H$  and  $\Delta S$  values (Table 1) between **D4** and **T1** suggest that the phosphate group on pS and the phenyl group on F at P+3 are the major contributors to BRCT binding.

Replacing the pyrrolidine ring of the Pro with the Ala side chain results in an increased  $\Delta H$  of **T2** compared to the parent peptide **T1** which is consistent with the availability of an extra H-bond donor ( $\alpha$ -N on Ala). The loss of conformational freedom (Pro to Ala) corresponds well with the increased unfavorable entropy ( $\Delta\Delta S = +7.3$  cal/(mol K)) of **T2** compared to **T1**. On the other hand **T3** and **T1** peptides have the same backbone with the hydroxyl group (Thr) on **T1** as a potential hydrogen bond donor/acceptor. The crystal structure data of the complex (1T29) shows (a) no protein contacts with the Thr (P+2) residue of the dodecapeptide peptide and (b) presence of two uncoordinated water molecules (WAT 45 and WAT 63) within 4 Å distance from the Thr side chain.<sup>4</sup> Therefore, we expected the difference in the binding affinities between peptides **T3** and **T1** to correlate predominantly with a decrease in  $\Delta H$  of **T3** and little to no change in the  $\Delta S$ . However,

the observed signature shows an increase in the  $\Delta H$  and a surprisingly larger unfavorable entropy ( $\Delta\Delta S = +19$  cal/(mol K)) of **T3** compared to **T1** (Table 1). Such changes in enthalpy have been shown to be associated with solvent reorganization, changes in hydrophobicity, and change in packing volume.<sup>8</sup> The later two changes would be reasons for the bumping/weakening of Phe association with its hydrophobic site on BRCT owing to Ala substitution (P+2) in **T3**.

Alternatively, this also suggests that the hydroxyl group of Thr side chain may be involved in intramolecular hydrogen bonding that contributes to conformational rigidity of the tetrapeptide **T1** for efficient tethering. Therefore the removal of the hydroxyl group by Ala substitution in **T3** eliminates the intramolecular hydrogen bonding making it more flexible resulting in the observed increase in the entropy ( $\Delta\Delta S = +19$  cal/(mol K)). Also this change facilitates intermolecular hydrogen bonding with the protein which correlates well with the increase in the enthalpy ( $\Delta\Delta H = -4.0$  kcal/mol). On the basis of the available crystal structure we hypothesize that the Thr side chain in **T1** could potentially make intramolecular hydrogen bonds with the backbone –NH of the P+4 residue and the backbone –CO of the pS (Figure 1).

In summary, we have used two complementary techniques (FP and ITC) to define a tetrapeptide as a lead for a peptidomimetic based inhibitor design. More importantly both ITC and FP studies show that all four residues contribute to BRCT binding. We have also identified a potential hydrophobic site close to the motif that can be exploited to improve potency. The ITC studies in conjunction with the structural data suggest the presence of intramolecular hydrogen bonding that could bias the pSPTF peptide to adopt the bound conformation for efficient BRCT tethering.

**Acknowledgment.** Financial support by UTMB and ACS-IRG-96-152-07, Dr. J.C. Lee for VP–ITC instrument, and Dr. K. Rajarathnam for helpful discussions are gratefully acknowledged.

**Supporting Information Available:** Experimental procedures and results of FP, ITC, and docking studies. This material is available free of charge via the Internet at <http://pubs.acs.org>.

## References

- (1) Marcotte, E. M.; Pellegrini, M.; Ng, H. L.; Rice, D. W.; Yeates, T. O.; Eisenberg, D. *Science* **1999**, *285*, 751–3.
- (2) Tesmer, J. J. *Science* **2006**, *312*, 377–8.
- (3) (a) Cantor, S. B.; Bell, D. W.; Ganesan, S.; Kass, E. M.; Drapkin, R.; Grossman, S.; Wahrer, D. C.; Sgroi, D. C.; Lane, W. S.; Haber, D. A.; Livingston, D. M. *Cell* **2001**, *105*, 149–60. (b) Manke, I. A.; Lowery, D. M.; Nguyen, A.; Yaffe, M. B. *Science* **2003**, *302*, 636–9. (c) Yu, X.; Chini, C. C.; He, M.; Mer, G.; Chen, J. *Science* **2003**, *302*, 639–42. (d) Yu, X.; Chen, J. *Mol. Cell. Biol.* **2004**, *24*, 9478–86. (e) Wang, B.; Matsuoka, S.; Ballif, B. A.; Zhang, D.; Smorzewska, A.; Gygi, S. P.; Elledge, S. J. *Science* **2007**, *316*, 1194–1198.
- (4) (a) Clapperton, J. A.; Manke, I. A.; Lowery, D. M.; Ho, T.; Haire, L. F.; Yaffe, M. B.; Smerdon, S. J. *Nat. Struct. Mol. Biol.* **2004**, *11*, 512–8. (b) Botuyan, M. V.; Nomine, Y.; Yu, X.; Juranic, N.; Macura, S.; Chen, J.; Mer, G. *Structure (Cambridge, MA)* **2004**, *12*, 1137–46. (c) Shiozaki, E. N.; Gu, L.; Yan, N.; Shi, Y. *Mol. Cell* **2004**, *14*, 405–12. (d) Williams, R. S.; Lee, M. S.; Hau, D. D.; Glover, J. N. *Nat. Struct. Mol. Biol.* **2004**, *11*, 519–25. (e) Varma, A. K.; Brown, R. S.; Birrane, G.; Ladias, J. A. *Biochemistry* **2005**, *44*, 10941–6. (f) Glover, J. N.; Williams, R. S.; Lee, M. S. *Trends Biochem. Sci.* **2004**, *29*, 579–85.
- (5) (a) Lokesh, G. L.; Rachamalla, A.; Kumar, G. D.; Natarajan, A. *Anal. Biochem.* **2006**, *352*, 135–41. (b) Rodriguez, M.; Yu, X.; Chen, J.; Songyang, Z. *J. Biol. Chem.* **2003**, *278*, 52914–8.
- (6) Williams, R. S.; Green, R.; Glover, J. N. *Nat. Struct. Mol. Biol.* **2001**, *8*, 838–42.
- (7) (a) Fraczkiewicz, R.; Braun, W. *J. Comp. Chem.* **1998**, *19*, 319. (b) Muralidhara, B. K.; Negi, S.; Chin, C. C.; Braun, W.; Halpert, J. R. *J. Biol. Chem.* **2006**, *281*, 8051–61.
- (8) Baldwin, E.; Baase, W. A.; Zhang, X.; Feher, V.; Matthews, B. W. *J. Mol. Biol.* **1998**, *277*, 467–85.
- (9) DeLano, W. L. *The PyMol User's Manual*; DeLano Scientific LLC: San Carlos, CA, 1998.

JA0739178